Unidirectional recruitment is essential for viral latency

Ido Lavi[#], Supriya Bhattacharya[#], Ola Orgil, Ankita Awase, Nir Avital, Guy Journo, Vyacheslav Gurevich and Meir Shamay*

Daniella Lee Casper Laboratory in Viral Oncology, Azrieli Faculty of Medicine, Bar-Ilan University, Safed, Israel 1311502

[#] These authors contributed equally to this work

* Corresponding author

Meir Shamay

Email: meir.shamay@biu.ac.il

Running Title: Unidirectional recruitment of LANA by MeCP2

Author Contributions: Conceived and designed the experiments: I.L., S.B., M.S. Performed the experiments: I.L., S.B., A.A, Analyzed the data: I.L., S.B., G.J. & M.S. Generated tools & reagents: O.O., N.A., V.G., S.B., Wrote the paper: M.S.

Preprint Servers:

Classification: Biological sciences, Microbiology.

Competing Interest Statement: The authors declare no competing financial interests.

Keywords: CRISPR/Cas9, dCas9, KSHV, HHV-8, LANA, MeCP2, Recruitment.

Abstract

Kaposi's sarcoma associated herpesvirus (KSHV, HHV-8) is associated with several human malignancies. During latency the viral genomes reside in the nucleus of infected cells as large non-integrated plasmids, known as viral episomes. All KSHV infected cells express LANA, and LANA is essential for viral latency. LANA binding to the viral episomes is critical both for replication of the viral genomes during latency, and for tethering the viral episomes to the cell chromosomes during cell division. Directional recruitment of protein complexes are critical for proper function of many nuclear processes. To test for recruitment directionality between LANA and cellular proteins we directed LANA via catalytically inactive Cas9 (dCas9) to a repeat sequence to obtain easily detectable dots. Then, recruitment of nuclear proteins to these dots can be evaluated. We found that LANA recruited its known interactors ORC2 and SIN3A. Interestingly, LANA was unable to recruit MeCP2, but MeCP2 recruited LANA. Similarly, histone deacetylase 1 (HDAC1) that interact with the transcriptional-repression domain (TRD) of MeCP2, same as LANA, was unable to recruit MeCP2, but MeCP2 was able to recruit HDAC1. In contrast, HP1α that interacts with MeCP2 through a different domain, was able to recruit MeCP2. We propose that available interacting domains in DNA bound/dimerized form of MeCP2, forces this recruitment directionality. We found that cells derived from Rett syndrome and express a mutant MeCP2 (T158M), impaired in DNA binding, cannot support KSHV genome maintenance. Therefore, this unidirectional recruitment of LANA by MeCP2 identified MeCP2 as a critical factor for viral maintenance.

Significance Statement

Using a CRISPR/Cas9 recruitment assay, we show that some interacting proteins have a unidirectional recruitment property, where only one of the proteins can recruit its partner. We found unidirectional recruitment relations between the methylated DNA binding protein MeCP2 and KSHV encoded LANA. Where MeCP2 recruits LANA, but LANA is unable to recruit MeCP2. Similarly, MeCP2 recruits histone deacetylase 1 (HDAC1), but HDAC1 is unable to recruit MeCP2. We propose that this unidirectional recruitment is the result of available interacting domains. Furthermore, this unidirectional recruitment seems to be critical for viral latency, since LANA fails to maintain the viral genomes in MeCP2 mutant cells. Therefore, in this case unidirectional recruitment is a matter of survival or extinction.

Introduction

Kaposi's sarcoma associated herpesvirus (KSHV, HHV-8) is the causative agent of all forms of Kaposi's sarcoma (KS), and is tightly associated with primary effusion lymphoma (PEL), and multicentric

54 Castleman's disease (1, 2). Like all herpes viruses KSHV has two phases: latent (dormant) and lytic
55 (productive) cycle. During latency the viral genomes reside in the nucleus of infected cells as large non-
56 integrated plasmids, known as viral episomes. All KSHV infected cells express LANA, and LANA is
57 essential for viral latency (3-5). LANA binding to the viral episomes is critical both for replication by
58 recruitment of the cellular replication machinery to the viral genomes (6, 7), and for maintenance by
59 tethering the viral episomes to the cell chromosomes during cell division (8, 9). Both the N and C-terminal
60 regions of LANA have been shown to mediate chromosome association; the N-terminal via binding to core
61 histones H2A and H2B (10), while for the C-terminal several candidates were identified including MeCP2,
62 DEK and RING3 (11-13). Multiple LANA binding sites (LBS1 and LBS2) (14, 15) within the KSHV
63 terminal repeats, and its oligomerization ability (16, 17) create clearly visible LANA dots in KSHV-infected
64 cells. In contrast, LANA is equally distributed in the nucleus when it is expressed in un-infected cells. So,
65 it is challenging to determine whether LANA or the viral genomes are the recruiters of cellular factors.

66 For many nuclear processes directional recruitment of protein complexes is critical for proper function.
67 Transcription factor that binds a specific DNA sequence recruits co-activators and general transcription
68 factors that results in subsequent recruitment of RNA polymerase leading to gene expression. In this
69 scenario, it is expected that a transcription factor of interest will recruit the co-activator. However, the co-
70 activator that is recruited by other transcription factors as well, should not recruit the transcription factor of
71 interest. One example of recruitment directionality is the estrogen receptor, where the combination of ligand
72 binding, dimerization and sequence specific DNA binding are required to generate high affinity surface to
73 recruit co-activator proteins (18). This conformational change upon DNA binding and dimerization will
74 favor binding and recruitment of co-activator to enhancer/promoter bound receptor and minimize
75 interaction with DNA-free receptor.

76 MeCP2 binds methylated DNA and recruits co-repressor complexes to execute the readout of CpG
77 methylation into transcription repression (19). Several studies detected interaction between MeCP2 and
78 histone deacetylase 1 (HDAC1), and recruitment of histone deacetylase activity plays a role in transcription
79 repression imposed by MeCP2 (20, 21). MeCP2 and HDAC1 represent an example of two proteins that
80 interact in the nucleus. While MeCP2 recruits HDAC1 to methylated regions in order to repress
81 transcription, we expect that HDAC1 should not recruit MeCP2 to promoters in those cases where HDAC1
82 is recruited by other transcription factors. Another protein that plays important role in transcription
83 repression is heterochromatin protein 1 (HP1). HP1 interacts with the repressive mark histone 3 lysine 9
84 tri-methylation (H3K9Me3) and via recruitment of SUV39H1, the histone H3K9Me3 methyltransferase,

85 leads to spreading of this heterochromatin repressive histone mark (22, 23). HP1 has been shown to interact
86 with MeCP2 (24, 25), but whether HP1 can recruit MeCP2 is an open question.

87 Cas9 is an endonuclease that can be directed to different DNA targets that are complimentary to a guide
88 RNA and contain a PAM sequence (26). Soon after the discovery of this property, many applications of
89 this sequence specific targeting of Cas9 emerged. For targeting purposes, the endonuclease is no longer
90 needed, and a catalytically dead mutant Cas9 (dCas9) that still retains DNA binding capability was created
91 (26, 27). Targeting this dCas9 to promoter sequences results in transcription activation or repression
92 depending on the fused domains and the targeting location relative to the transcription start site (27, 28).
93 Shortly after the creation of the dCas9 it was directed to repeat elements for the visualization of these
94 elements in fixed (29) and live cells (30-32).

95 Here we harness CRISPR/Cas9 to determine recruitment relations between LANA and cellular proteins.
96 We termed this method CRISPR-PITA, for Protein Interaction and Telomere recruitment Assay. We
97 combined the ability of the SunTag system (33) to gather up to ten molecules of a protein of interest with
98 CRISPR/dCas9 targeted to a repeat sequence such as telomeres. The ability of this protein to recruit
99 endogenous or fluorescently tagged proteins to these telomere dots is determined. Interestingly, we find
100 that the recruitment does not always work bi-directionally. LANA fails to recruit MeCP2, but MeCP2
101 efficiently recruits LANA. The unidirectional recruitment of LANA by MeCP2 raised the possibility that
102 MeCP2 may serve as a protein anchor for LANA tethering. Indeed, we found that the virus fails to maintain
103 its episomes in cells expressing a mutant MeCP2. We hypothesized that the interaction domain will only
104 become available for interaction with LANA upon binding to DNA. To test this, we performed recruitment
105 assay of MeCP2 by LANA in the presence of a short DNA oligo with MeCP2 binding site. Interestingly,
106 now LANA was able to recruit MeCP2. We propose that available interacting domains can determine
107 recruitment directionality.

108

109 **Results**

110 **Creation of visible dots at the telomeres with dCas9-SunTag and scFv-LANA**

111 The KSHV encoded LANA localizes in large dots together with the viral episomes in KSHV infected cells
112 but is equally distributed in the nucleus when expressed in un-infected cells (34). In order to test recruitment
113 directionality between LANA and nuclear proteins we were interested to create LANA dots in un-infected
114 cells. The ability of dCas9 to direct proteins of interest to any genomic locus makes it an ideal system for a
115 recruitment assay. In order to enhance dot formation, we utilized the SunTag system where tandem epitopes

116 can concentrate multiple molecules of an antibody-fused protein that recognizes this epitope (up-to 10 with
117 the tag used in this study) (33). In our case the tandem epitopes are fused to dCas9 and the antibody scFv
118 is fused to our protein of interest (**Fig. 1A**). Transfection of LANA fused with the antibody scFv (scFv-
119 LANA) together with dCas9 and sgRNA for telomere repeat sequence, resulted in LANA-telomere-dots
120 that were visible by immuno-fluorescent assay (IFA) for LANA (**Fig. 1B**). When the dCas9 was omitted
121 from the mix LANA could not generate nuclear dots, suggesting that LANA-telomere-dots are dependent
122 on the targeting of LANA to telomeres via dCas9. To validate that LANA was targeted to the telomeres we
123 used an antibody against the telomeric repeat factor 2 (TRF2), and indeed scFv-LANA co-localized with
124 TRF2 when co-transfected with dCas9 and sgTelomere (**Fig. S1**). The larger dots of TRF2 observed where
125 it colocalize with LANA, can be explained by LANA's ability to oligomerize (14, 16, 17, 35, 36). Studies
126 of the LANA oligomerization property identified a LANA oligomerization mutant (16, 17). Therefore, we
127 created this LANA oligomerization mutant (F1037A/F1041A) in the context of scFv-LANA (scFv-LANA-
128 mutant) and compared the dot size to scFv-LANA. As expected, the LANA oligomerization mutant created
129 smaller telomere dots compared to wt LANA of both LANA and TRF2 (**Fig. S1**). Altogether, these
130 experiments indicate that we can generate LANA dots in un-infected cells using the dCas9 SunTag system.

131 **LANA recruits ORC2 and SIN3A but not MeCP2**

132 In this assay a protein of interest is targeted to telomeres via dCas9, and the recruitment of endogenous
133 proteins to these dots is detected by immunofluorescence assay (**Fig. 1C**). We termed this method CRISPR-
134 PITA for Protein Interaction and Telomere recruitment Assay. We performed the CRISPR-PITA assay for
135 ORC2, a subunit of the Origin Replication Complex (ORC), previously reported to interact with LANA
136 and localize with LANA-episome-dots (17, 37-39). ORC2 was recruited by LANA, as was determined by
137 the easily detected dots that co-localized with LANA (**Fig. 2A**), and the overlapping fluorescence intensity
138 peaks along the arrow line (on the right side of the images). It is important to note, that while the dCas9 and
139 scFv-LANA were ectopically expressed, the recruited proteins are endogenous proteins, indicating the
140 ability of LANA to recruit the endogenous ORC2.

141 Several studies reported on interaction between LANA and the corepressor protein SIN3A (mSin3a) (39,
142 40), and the methyl-CpG binding protein MeCP2 (11, 12, 41), but it was reported that MeCP2 is not
143 associated with LANA dots in KSHV infected cells (42). We found that scFv-LANA recruited SIN3A to
144 LANA-telomere-dots, both by the visual observation of the dots and the fluorescence intensity plot (**Fig.**
145 **2B**). Analysis of MeCP2 recruitment via the CRISPR-PITA revealed no recruitment of MeCP2 to LANA-
146 telomere-dots (**Fig. 2C**). We also determined the Pearson's correlation coefficient for the different

147 treatments (**Fig. 2D**). When LANA alone is transfected, there should be an overlap between LANA and
148 these proteins, as they are known LANA interactors. When LANA is targeted to the telomeres via dCas9,
149 if LANA is able to recruit its partner, then the overlap is expected to remain or even increase. In contrast,
150 if LANA is unable to recruit its partner, the overlap should be reduced. This is exactly what we found when
151 we measured the Pearson's correlation coefficient for 15 cells in each experiment. The overlap was reduced
152 for the non-recruited MeCP2, remained the same for SIN3A, and increased for ORC2.

153 One possibility to explain the lack of MeCP2 recruitment by LANA, is that as a methylated DNA binding
154 protein, it is engaged in binding methylated DNA and therefore not available to be recruited by LANA. To
155 test this, we performed the CRISPR-PITA in cells with knock-out (KO) of DNMT1 and DNMT3b (HCT
156 DKO) that were reported to lose over 95% of their CpG methylation (43). Even in HCT DKO, scFv-LANA
157 could not recruit MeCP2 to LANA-telomere-dots (**Fig. S2**), suggesting that protein availability could not
158 explain the lack of recruitment in this case. Immunofluorescence assays for ORC2, SIN3A and MeCP2 in
159 KSHV-infected PEL (BCBL1) cells, revealed that while ORC2 and SIN3A were found associated with
160 LANA-episome-dots, MeCP2 was not associated with the LANA-episome-dots (**Fig. S3**), supporting the
161 ability of the CRISPR-PITA to predict recruitment ability between proteins.

162 **MeCP2 recruits LANA**

163 The observation that scFv-LANA could not recruit MeCP2, despite their documented interaction (11, 12,
164 41) highlights the importance to determine recruitment relations between proteins. Krithivas et al. have
165 shown that expression of human MeCP2 is able to recruit LANA to heterochromatin in NIH 3T3 mouse
166 cells (12). Therefore, we tested the ability of scFv-MeCP2 to recruit LANA to MeCP2-telomere-dots. Cells
167 were co-transfected with dCas9, sgTelomere, scFv-MeCP2 and expression vectors for GFP-LANA or GFP
168 alone as control. The scFv-MeCP2 was able to recruit GFP-LANA to MeCP2-telomere-dots, but not GFP
169 alone, supporting the ability of MeCP2 to recruit LANA (**Fig. 3A & B**). LANA contains three distinct
170 domains, the N-terminal region (AA 1-329), the C-terminal (AA 936-1162), and a middle repeat region.
171 Both the N and C-terminal regions have been shown to mediate chromosome association; the N-terminal
172 via binding to core histones H2A and H2B (10), while for the C-terminal several candidates were identified
173 including MeCP2, DEK and RING3 (11-13). To determine the region of LANA sufficient for recruitment
174 by MeCP2, we performed CRISPR-PITA by scFv-MeCP2 for LANA N+C, LANA N and LANA C. While
175 both LANA N+C and LANA C were efficiently recruited by MeCP2, no recruitment was observed with
176 the N-terminal (**Fig. 3C**). This result agrees with a previous study that located the interaction between
177 LANA and MeCP2 to the C-terminal region (11). Importantly, this result indicates that despite the high

178 concentration of the recruiter protein at telomeres, still CRISPR-PITA requires specific interaction, as both
179 the N-terminal of LANA and GFP-alone were not recruited by MeCP2 in our assay.

180 Targeting dCas9 to a repeat element, results in high protein concentration at specific nuclear locations. One
181 concern that might be raised is whether the recruitment we observed with CRISPR-PITA is specific or an
182 artifact of the high protein concentration. To rule out this possibility, we directed dCas9 to a single
183 chromosomal location (at ERBB2 promoter) and followed the association of the proteins with this location
184 by chromatin immunoprecipitation (ChIP) assay followed by qPCR (**Fig. 3D**). Here again we found that
185 scFv-MeCP2 recruited more LANA to this promoter, while scFv-LANA failed to do the same for MeCP2.
186 This result indicates that despite targeting dCas9 to a repeat sequence, the recruitment nicely reflects the
187 recruitment by a single locus. This set of experiments highlights the distinction between interaction and
188 recruitment, while LANA and MeCP2 were shown to interact with each other, still MeCP2 can recruit
189 LANA, but LANA cannot recruit MeCP2.

190 **MeCP2 recruits HDAC1, but HDAC1 is unable to recruit MeCP2**

191 Several studies detected interaction between MeCP2 and histone deacetylase 1 (HDAC1), and this
192 recruitment of histone deacetylase activity plays a role in transcription repression imposed by MeCP2 (20,
193 21). MeCP2 and HDAC1 represent an example where two proteins can interact to form protein complexes
194 in the nucleus. We expect that MeCP2 should recruit HDAC1 to methylated regions in order to repress
195 transcription, but HDAC1 should not recruit MeCP2 to the promoters where it is recruited by other
196 transcription factors. Therefore, we applied the CRISPR-PITA to determine recruitment relations between
197 these two cellular proteins. We found that scFv-MeCP2 efficiently recruits HDAC1 (**Fig. 4A**). In contrast,
198 scFv-HDAC1 failed to recruit MeCP2 both in HCT (**Fig. 4B**) and HCT DKO cells (**Fig. 4C**). Thus, in the
199 context of MeCP2 and HDAC1, recruitment is also unidirectional, enabling MeCP2 to recruit HDAC1 to
200 repress transcription, but preventing the mislocalization of MeCP2 by HDAC1.

201 **Availability of interacting domains determines recruitment directionality**

202 A unidirectional recruitment between two interacting proteins is achieved when the interacting domain is
203 available only upon certain conditions. In the case of MeCP2, it is expected that the transcriptional-
204 repression domain (TRD) will be unavailable when it is a free protein in solution and becomes available
205 for protein interaction only when MeCP2 is bound to DNA (**Fig. 5 C-D**). Both LANA and HDAC1 interact
206 with the same region of MeCP2, the transcriptional-repression domain (TRD) and the methyl-CpG-binding
207 domain (MBD) (35, 40). In contrast, Heterochromatin protein 1 (HP1α) interacts with the N-terminal

208 domain (amino acids 1–55) of MeCP2 (24) (**Fig. 5A**). We hypothesized that since HP1α interacts with a
209 different domain that might be available for interaction also in its DNA-free state, HP1α might be able to
210 recruit MeCP2. Interestingly, in CRISPR-PITA we found that scFv-HP1α was able to recruit MeCP2 (**Fig.**
211 **5B**).

212 This result supports the notion that available interacting domains determine recruitment directionality. To
213 test this more directly, we performed recruitment assay of MeCP2 by scFv-LANA but now also provided
214 a short double-strand (ds) DNA oligo with MeCP2 binding site. If our model is correct, MeCP2 will bind
215 the oligo, make the interaction domain with LANA available, but now instead of binding cellular chromatin,
216 it is bound to a short oligo and therefore can move around and be recruited by LANA. This is exactly what
217 we observed when we transfected a short DNA oligo with MeCP2 binding site (**Fig. 5 E-F**). No recruitment
218 was observed in un-transfected cells or cells transfected with a control DNA. This result supports the notion
219 that LANA can interact only with a DNA bound MeCP2.

220 **Rett syndrome mutant MeCP2 cannot support KSHV maintenance during latency**

221 One important function of LANA is to maintain the viral episomal genomes, by tethering the viral genomes
222 to cellular chromosomes during cell division, ensuring they remain in the nucleus once nuclear envelope is
223 reformed. To do so, LANA directly binds the LANA binding sites (LBS1 and LBS2) (14, 15) on the viral
224 genomes, and associates with cellular chromosomes. Our finding that MeCP2 recruits LANA, while LANA
225 cannot recruit MeCP2 unless we provide a short oligo with MeCP2 binding site, suggests that the interaction
226 with MeCP2 is permitted only once it is bound to methylated DNA, and therefore may be a potential
227 candidate for LANA tethering. Sporadic mutations in MeCP2 are associated with most cases of Rett
228 syndrome (RTT), a severe X-linked neurodevelopmental disorder in humans. (44). Lymphoblastoid Cell
229 Lines (LCLs) derived from RTT patients expressing wild-type (wt) MeCP2 allele, mutant T158M (that
230 cannot bind methylated DNA), and 803delG (deletion of the C' terminus) (**Fig. 5A**) of MeCP2 (45) were
231 tested for their ability to support KSHV episome maintenance. Cells were infected with rKSHV
232 (rKSHV.219) expressing GFP and maintenance of the viral episomal DNA and the percentages of GFP
233 positive cells were analyzed (**Fig. 6 B & A**). While both wt and 803delG efficiently supported viral latency,
234 the MeCP2 mutant in the MBD that cannot bind DNA (T158M) could not. This result indicates that a
235 functional MeCP2 that is able to bind methylated DNA is essential for KSHV genome maintenance. LANA
236 has been shown to bind both the MBD and TRD of MeCP2 (11). To determine if LANA can be recruited
237 by the T158M mutant, we cloned it into scFv-MeCP2 and performed CRISPR-PITA assay. We found that
238 MeCP2 T158M mutant can recruit LANA (although to a lesser extent), when it is artificially targeted to

239 chromatin by dCas9 (**Fig. 6C**). While the MBD deletion mutant, lost the ability to recruit LANA when
240 artificially targeted to chromatin. To assay for both abilities, to recruit LANA and to bind methylated DNA,
241 we harnessed a specific feature of MeCP2 to localize to heterochromatin loci in mouse cells. This assay is
242 typically performed in NIH 3T3 cells, since they express very low levels of endogenous MeCP2 (12, 46).
243 Similar to previous studies (11, 12), we found that LANA can be efficiently recruited to heterochromatin
244 when co-transfected with wt MeCP2 (**Fig. 6D**). In contrast, both T158M and MBD-del mutants could not
245 recruit LANA to heterochromatin loci. Altogether, we found that Rett syndrome mutant MeCP2 T158M,
246 that cannot recruit LANA to methylated DNA, also cannot support KSHV episome maintenance. We
247 revealed a critical role for MeCP2 in KSHV episome maintenance by LANA.

248 **Discussion**

249 A powerful method to study recruitment is the Chromatin immunoprecipitation (ChIP) assay, that can detect
250 association of proteins with specific DNA sequences (47, 48). ChIP assays require fixation, proper shearing
251 of the chromatin, and special antibodies that can perform the immunoprecipitation of the cross-linked
252 chromatin. In many cases even when two or more proteins are associated with the same genomic region, it
253 is hard to evaluate the relationship between the proteins and determine essential factors for the recruitment.
254 Although this limitation can be overcome by using Knockout (KO) or Knockdown (KD) of one protein and
255 testing the ability of other proteins to be recruited to DNA/chromatin in the absence of that protein, this
256 raises additional challenges in creating KO or KD of the target gene. Another recruitment assay is based
257 on integration of the *lac*O array into the genome and directing the protein of interest to this array via fusion
258 to the Lac-repressor (49, 50). One limitation of this assay is the limited number of cell lines that were
259 generated to contain integration of this *lac*O array.

260 Here we describe a simple method to test for recruitment relations between proteins. This method does not
261 require chromatin shearing and can be performed with various antibodies that can recognize the native form
262 of proteins, and in the absence of such an antibody a recruitment of fluorescently labeled proteins can be
263 observed. To obtain visible dots we combined the ability of the repeated epitope SunTag with dCas9
264 targeted to a repetitive genomic sequence such as the telomeres. Although targeting dCas9 to telomeres has
265 been performed previously to follow nuclear events such as, liquid–liquid phase separation (LLPS), or the
266 generation of heterochromatin (51, 52), but has not been applied to test recruitment directionality. Using
267 this method, we found unidirectional recruitment relations between proteins. Our results with CRISPR-
268 PITA, indicated that LANA was able to recruit ORC2 and SIN3A, but was unable to recruit MeCP2 to
269 LANA-telomere-dots. While it has been shown that ORC2 localizes with LANA dots (17, 37-39), and
270 MeCP2 does not (42), there was no published data on SIN3A localization in KSHV infected cells. So, we

271 performed immunofluorescence assay in KSHV-infected BCBL1 cells and found that both ORC2 and
272 SIN3A were associated with LANA dots, but MeCP2 was not. The immunofluorescence assays in KSHV-
273 infected cells are in agreement with the CRISPR-PITA results, supporting the ability of CRISPR-PITA to
274 predict recruitment ability of proteins. While both ORC2 and SIN3A were recruited by LANA in CRISPR-
275 PITA, it seems that ORC2 was recruited to most LANA dots, while SIN3A was associated only with part
276 of LANA dots. This difference was also reflected in the Pearson's correlation coefficient, where the
277 correlation with SIN3A remained the same while the correlation with ORC2 increased upon directing
278 LANA to telomeres. Interestingly, this difference was also observed in infected cells, where SIN3A seems
279 to colocalize with only part of LANA-episome dots. The recruitment of GFP-LANA by scFv-MeCP2 also
280 suggests that CRISPR-PITA can be done without cell fixation or immunofluorescence, but directly via
281 detection of fluorescently-labeled proteins. This property might be more relevant in cases where CRISPR-
282 PITA is applied for screening purposes.

283 Targeting dCas9 to a repeat element, results in high protein concentration at specific nuclear locations. One
284 concern that might be raised is whether the recruitment we observed with CRISPR-PITA is specific or an
285 artifact of the high protein concentration. Our result that the same recruitment relations are detected also
286 when we directed dCas9 to a single locus (ERBB2 promoter), rules out this possibility. Regarding
287 specificity, we found that scFv-MeCP2 recruited the C-terminal of LANA, but not its N-terminal.
288 Interaction of LANA C-terminal domain with MeCP2 is in agreement with a previous study for LANA
289 (11). The related gamma-2 herpesvirus, herpesvirus saimiri (HVS) encodes for ORF73, a functional
290 homolog of KSHV encoded LANA (also known as ORF73). Interestingly, also HVS encoded ORF73
291 interacts with MeCP2 via its C-terminal domain (46). The lack of recruitment for the N-terminal domain of
292 LANA, indicated that recruitment is still specific and requires the interaction domain. Another support for
293 the specific recruitment by CRISPR-PITA is the lack of recruitment observed for GFP alone. A growing
294 list of nuclear proteins with intrinsically disordered regions and RNA/DNA binding properties can promote
295 liquid–liquid phase separation (LLPS); both LANA and MeCP2 possess this property (53, 54). Rett
296 syndrome MeCP2 mutants, including T158M are impaired in LLPS formation. Since T158M mutant still
297 can recruit LANA in CRISPR-PITA (although to a lesser extent), indicates that the recruitment we observed
298 is not dependent on LLPS formation.

299 The inability of LANA to recruit MeCP2, despite their documented interaction prompted us to test whether
300 MeCP2 can recruit LANA. Indeed, in CRISPR-PITA scFv-MeCP2 was able to recruit LANA. This result
301 comes in agreement with a previous study where MeCP2 recruited LANA to mouse heterochromatin foci
302 (12). This result also highlights the importance of a recruitment assay as recruitment is not always bi-

303 directional, and in many cases should be functionally unidirectional. One of LANA functions where
304 unidirectional recruitment seems essential, is LANA tethering of the viral episomal genome to the cell
305 chromosomes during cell division. Therefore, we tested the possible role of MeCP2 in KSHV episome
306 maintenance. We found that Rett syndrome mutant MeCP2, that cannot bind methylated DNA (T158M),
307 could not support KSHV latency. Our result suggests that in addition to LANA interaction with histones
308 (10), MeCP2 adds another layer to secure chromosome tethering (suggested model in **Fig. S4**). Similar to
309 KSHV encoded LANA, HVS encoded ORF73 has a critical role in viral episomal genome maintenance
310 (55). MeCP2 has been shown to be essential for tethering of the viral genomes by ORF73 to maintain HVS
311 latency (46). Therefore, our observation that MeCP2 is essential for episome maintenance, seems to be
312 conserved between KSHV and HVS. In this scenario LANA/ORF73 binds MeCP2 to anchor the viral
313 episomes to cellular chromosomes. If the anchor (MeCP2) is free (not bound to DNA/chromosome), this
314 may lead to viral loss. Therefore, in this case unidirectional recruitment is a matter of survival or extinction.

315 Do Rett syndrome patients are resistant to KSHV viral latency? *MeCP2* gene is located on the X-
316 chromosome, and Rett syndrome is found almost exclusively in females. Females, inherent two copies of
317 X-chromosome, one maternal and one paternal. During development one X-chromosome, is subjected to
318 X-chromosome inactivation, allowing expression of only one copy. Since females will present a mosaic
319 expression of the mutant and wt *MeCP2* alleles in different cells, it is reasonable to speculate that female
320 Rett syndrome patients will not be resistant to KSHV latent infection. It is important to note that in our
321 experiments, we used Single-cell derived clonal LCLs expressing either wt or mutant Rett syndrome
322 MeCP2 allele (45). Rett syndrome in males is very rare leading to in-utero lethality in most cases due to
323 having only a single copy of non-functional MeCP2. Another factor that contributes to the rarity of Rett
324 syndrome in males is their maternal origin of x-chromosome. While most MeCP2 mutations are sporadic,
325 and preferentially occur on the paternal x-chromosome (56, 57). So, only in these very rare cases of male
326 Rett syndrome, and only in those cases that the mutation disrupts DNA binding or the TRD domain of
327 MeCP2 we can expect a resistance to KSHV latency.

328 A nice example of directional recruitment is the case of MeCP2 that binds methylated DNA and recruits
329 co-repressor complexes including HDAC1 (20, 21). In this case we expect that MeCP2 should recruit
330 HDAC1, leading to transcription repression. On the other hand, HDAC1 is recruited by many transcription
331 factors to generate repressive chromatin. Therefore, we expect that it should not recruit MeCP2 to all the
332 chromosome locations it is recruited by other transcription repressors. Indeed, we found that scFv-MeCP2
333 was able to recruit HDAC1 to MeCP2-telomere-dots, but scFv-HDAC1 was unable to recruit MeCP2. How
334 come two proteins that interact with each other can generate unidirectional recruitment? MeCP2 is an

335 intrinsically disordered protein that is monomeric in solution even at high concentrations but dimerizes
336 upon DNA binding (58, 59). Although CRISPR-PITA does not directly test the DNA binding of MeCP2,
337 however the SunTag brings several MeCP2 molecules together therefore might force dimerization or
338 binding to a DNA nearby, and by that can mimic DNA bound MeCP2. This might explain how the mutant
339 MeCP2 T158M partially recruits LANA in CRISPR-PITA. Both LANA and HDAC1 interact with the
340 MBD and TRD of MeCP2 (11, 21). In contrast, HP1α interacts with the N-terminal domain (amino acids
341 1–55) of MeCP2 (24). Therefore, while the TRD domain should be available for interaction only upon DNA
342 binding and MeCP2 dimerization, we predicted that the N-terminal domain might be available for
343 interaction also in its DNA-free form. Indeed, we found that HP1α is able to recruit MeCP2 to HP1α-
344 telomere-dots. Another prediction of the model is that in the presence of a small DNA oligo for MeCP2
345 binding site, MeCP2 will bind the oligo, the interaction domain will become available and MeCP2 will be
346 recruited by LANA. Indeed, in the presence of a small DNA oligo for MeCP2 binding site LANA was able
347 to recruit MeCP2. Based on these characteristics and our CRISPR-PITA results we propose the following
348 model; when MeCP2 is not associated with DNA it is a monomer and therefore the TRD and MBD are not
349 available to interact with HDAC1 and LANA and therefore cannot be recruited by them. When MeCP2
350 binds methylated DNA its conformation changes so the TRD and MBD can bind and recruit HDAC1 and
351 LANA. In this way, unidirectional recruitment of HDAC1 and LANA only to DNA bound MeCP2 is
352 executed, while interaction with free MeCP2 is prevented (**Fig. 5C & D**). On the contrary, HP1α interacts
353 with a different region, the N-terminus of MeCP2 that is available for binding also in its DNA-free state,
354 and therefore HP1α can recruit MeCP2. It has been shown that phosphorylation at serine 229 (pS229) of
355 MeCP2 strongly enhances the interaction between MeCP2 and HP1α (25). Our observation that HP1α can
356 recruit MeCP2, may explain their observation that MeCP2 pS229 was enriched at the receptor tyrosine
357 kinase gene *RET* promoter. In the future, it will be interesting to test the role of HP1α in the global
358 distribution of MeCP2.

359

360 **Materials and Methods**

361 **Cell culture**. SLK cells (kindly provided by Don Ganem & Rolf Renne), NIH 3T3 cells (kindly provided
362 by Oren Kobiler) and Vero-rKSHV.219 cells (kindly provided by Jeffrey Vieira) were cultured in
363 Dulbecco's modified Eagle's medium (DMEM) supplemented with 10% fetal bovine serum (heat
364 inactivated) and 100 U/ml penicillin, 100 μg/ml streptomycin, 2 mM L-glutamine, and 1 mM Sodium-
365 Pyruvate in 5% CO_2 at 37°C. HCT and HCT Dnmt1-/- Dnmt3b -/- (DKO) cells (kindly provided by Bert
366 Vogelstein) were grown in McCoy's 5A medium supplemented with the above-mentioned supplements.

367 BJAB and BCBL1 cells (kindly provided by Richard F. Ambinder), and LCLs (kindly provided by Uta
368 Francke), were cultured in RPMI-1640 medium supplemented with 20% FBS and the above-mentioned
369 supplements. Single-cell derived clonal LCLs expressing the wt or mutant Rett syndrome MeCP2 allele
370 were established in the lab of Uta Francke (45).

371 **Plasmids**. pHRdSV40-dCas9-10xGCN4_v4-P2A-BFP (Addgene plasmid # 60903;
372 http://n2t.net/addgene:60903; RRID:Addgene_60903) and pHR-scFv-GCN4-sfGFP-GB1-dWPRE
373 (Addgene plasmid # 60907; http://n2t.net/addgene:60907; RRID:Addgene_60907) were a gift from Ron
374 Vale (33). pgRNA-humanized was a gift from Stanley Qi (Addgene plasmid # 44248;
375 http://n2t.net/addgene:44248; RRID:Addgene_44248) (27). The sgRNA targeting telomeres was cloned
376 into pgRNA-humanized. The mCherry in the pgRNA-humanized was deleted by restriction digestion and
377 ligation. LANA, HDAC1, HP1α and MeCP2 were PCR amplified and cloned into pHR-scFv-GCN4-
378 sfGFP-GB1-dWPRE. scFv-LANA was further subcloned into pLIX_403, a gift from David Root (Addgene
379 plasmid # 41395; http://n2t.net/addgene:41395; RRID:Addgene_41395). pEGFP-c2 from Clontech. GFP-
380 LANA and LANA deletion plasmids were described previously (39, 60). For generation of MeCP2
381 (T158M) mutation RNA was isolated from LCL 487 (T158M) cell line by Qiagen RNeasy mini kit (cat no
382 # 79656) and cDNA was prepared by maxima H minus first strand cDNA synthesis kit (cat no # K1682).
383 A fragment of MeCP2 containing the T158M mutation was amplified by PCR and cloned in MeCP2-GFP
384 plasmid (Addgene # 48078) and subsequently cloned into pHR-scFv-GCN4-sfGFP-GB1-dWPRE plasmid.
385 MBD domain deleted MeCP2 was created by overlap extension PCR. Oligomerization mutant LANA was
386 created by Q5 site directed mutagenesis kit (cat no# NEB E0554S). All primers can be found in
387 supplementary primer list (**Table S1**). For ChIP assays we cloned the dCas9-5xSunTag from pCAG-dCas9-
388 5xPlat2AflD, a gift from Izuho Hatada (Addgene plasmid # 82560 ; http://n2t.net/addgene:82560 ;
389 RRID:Addgene_82560) (61), and sgRNA for ERBB2 promoter into lentiCRISPRv2 hygro, a gift from
390 Brett Stringer (Addgene plasmid # 98291 ; http://n2t.net/addgene:98291 ; RRID:Addgene_98291) (62).

391 **Immunofluorescence assay**. $1X10^5$ cells were plated in 12 wells plate. Next day the cells were washed
392 once with PBS and were transfected using PolyJet In Vitro DNA Transfection Reagent (SignaGene
393 Laboratories Cat # SL100688) with the appropriate plasmids. In the day after $4X10^4$ cells were transferred
394 into chamber slide cell culture glass 8 wells (SPL life Science LTD). Next day, the cells were washed once
395 with PBS followed by fixation in 4% paraformaldehyde in PBS pH 7.4 for 10 minutes. After 3 washes with
396 PBS, cells were permeabilized for 10 min with PBS containing 0.25% Triton X-100. Cells were washed 3
397 times with PBS and blocked with 1% BSA, 22.52 mg/mL glycine in PBST (PBS+ 0.1% Tween 20) for 45
398 min in 37° C. The slides were incubated for 1 hour with primary antibodies, followed by 3 washes with

399 PBS. Then, the slides were incubated with secondary antibodies for 1 hour and washed again 3 times with
400 PBS and mounted with Vectaschield containing DAPI (Vector Laboratories, H-1500).

401 **Antibodies**. The following antibodies were used for immunofluorescence studies: Rat anti LANA
402 (Advanced Biotechnologies, cat#13-210-100), Mouse anti LANA (Leica, NCL-HHV8-LNA), Mouse anti
403 TRF2 (Merck, 05-521), Rabbit anti MeCP2 (Abcam, ab2828), Rabbit anti mSin3a/SIN3A (Abcam,
404 ab3479), Mouse anti HA (Sigma H9658), Mouse anti ORC2 (MBL Life Science, M055-3), and Rabbit anti
405 HDAC1 (Abcam, ab53091). Goat anti rabbit Alexa 488 (Abcam, ab150077), Goat anti Rat Alexa 488
406 (Abcam, ab150157), and Goat anti Mouse Alexa 594 (Abcam, ab150116). scFv-MeCP2, scFv-HP1α, and
407 scFv-HDAC1 were detected with Mouse anti HA. scFv-LANA was detected by Mouse anti LANA, except
408 in combination with TRF2 where Rat anti LANA was used. FLAG-LANA mutants (N+C, N, C) were
409 detected with Rabbit anti FLAG (Sigma 7425).

410 **Confocal imaging.** Images were captured with Zeiss LSM780 inverted confocal microscope through a 63X
411 objective with Z stack mode. Then, the middle stacks were selected and merged using Subset mode and
412 Maximum Intensity Projection mode, respectively with Zenn software black edition. Processing and
413 exporting of the resulted images was done with Zenn software blue edition.

414 **Chromatin immunoprecipitation assay.** ChIP assays were performed as described previously (63).
415 Immunoprecipitation was performed with protein A/G Dynabeads (ThermoFisherScientific, #100-
416 02D/100-04D) bound with Rat anti-LANA (Advanced Biotechnologies, cat#13-210-100), Rabbit anti-
417 MeCP2 (Abcam, ab2828), or normal IgG (Millipore, PP64B) as a negative control. The immunoprecipitated
418 chromatin was washed five times (with NaCl, lithium chloride and Tris-EDTA buffers), eluted and then
419 purified using QIAquick kit (Qiagen, #28104) according to manufacturer's instructions.
420 **LCL infection and maintenance assay**. LCLs were infected with KSHV by co-culture (64). Briefly, Vero-
421 rKSHV.219 cells (45) were induced with 1.25 mM sodium butyrate and 20 ng/ml 12-*O*-
422 tetradecanoylphorbol-13-acetate (TPA) and after 48 h were cocultured with LCL cells (1:1 cell ratio) in
423 RPMI 1640 medium for an additional 48 h. Medium containing the LCLs infected cells was collected and
424 transferred to a new flask for an additional 48 h. Transferred again to a new flask, and at days 2, 7, 14, 24,
425 cells were taken for FACS analysis to detect the number of GFP positive cells. At the same time points,
426 genomic DNA was isolated with DNeasy blood and tissue kit (cat no # 69506) as per manufacturer
427 instructions. Real time PCR was performed on genomic DNA using Fast SYBR green master mix (Applied

428 Biosystems), and results were analyzed with a CFX96 Touch real-time PCR detection system (Bio-Rad).
429 GAPDH was used as an internal control.
430
431
432 **Data availability**
433 N.A. , as we did not generate large data sets.
434
435 **Funding**
436 This work was supported by grants from the Israel Science Foundation (https://www.isf.org.il) to M.S.
437 (1365/21), and Research Career Development Award from the Israel Cancer Research Fund
438 (https://www.icrfonline.org/) to M.S. (01282). We are grateful for the support of the Elias, Genevieve and
439 Georgianna Atol Charitable Trust to the Daniella Lee Casper Laboratory in Viral Oncology. The funders
440 had no role in study design, data collection and analysis, decision to publish, or preparation of the
441 manuscript.
442
443 **Acknowledgments**
444 We would like to thank J Ron Vale, Stanley Qi, David Root, Izuho Hatada, Brett Stringer, and S. Diane
445 Hayward for kindly providing plasmids, and Don Ganem, Rolf Renne, Jeffrey Vieira, Oren Kobiler,
446 Richard F. Ambinder, Bert Vogelstein and Uta Francke for cell lines. We also would like to thank S. Diane
447 Hayward for critically reading the manuscript, and Yosef Shaul for fruitful discussions.
448
449 **References**

450 1. Y. Chang *et al.*, Identification of herpesvirus-like DNA sequences in AIDS-associated
451 Kaposi's sarcoma. *Science (New York, N.Y* **266**, 1865-1869 (1994).
452 2. C. Henke-Gendo, T. F. Schulz, Transmission and disease association of Kaposi's sarcoma-
453 associated herpesvirus: recent developments. *Curr Opin Infect Dis* **17**, 53-57 (2004).
454 3. F. Ye, X. Lei, S. J. Gao, Mechanisms of Kaposi's Sarcoma-Associated Herpesvirus Latency
455 and Reactivation. *Adv Virol* **2011** (2011).
456 4. L. Rainbow *et al.*, The 222- to 234-kilodalton latent nuclear protein (LNA) of Kaposi's
457 sarcoma-associated herpesvirus (human herpesvirus 8) is encoded by orf73 and is a
458 component of the latency-associated nuclear antigen. *J Virol* **71**, 5915-5921 (1997).
459 5. D. H. Kedes, M. Lagunoff, R. Renne, D. Ganem, Identification of the gene encoding the
460 major latency-associated nuclear antigen of the Kaposi's sarcoma-associated herpesvirus.
461 *J Clin Invest* **100**, 2606-2610 (1997).
462 6. A. Grundhoff, D. Ganem, The latency-associated nuclear antigen of Kaposi's sarcoma-
463 associated herpesvirus permits replication of terminal repeat-containing plasmids. *J Virol*
464 **77**, 2779-2783 (2003).

465 7. J. Hu, A. C. Garber, R. Renne, The latency-associated nuclear antigen of Kaposi's sarcoma-
466 associated herpesvirus supports latent DNA replication in dividing cells. *J Virol* **76**, 11677-
467 11687 (2002).
468 8. B. Kelley-Clarke, E. De Leon-Vazquez, K. Slain, A. J. Barbera, K. M. Kaye, Role of
469 Kaposi's sarcoma-associated herpesvirus C-terminal LANA chromosome binding in
470 episome persistence. *J Virol* **83**, 4326-4337 (2009).
471 9. E. De Leon Vazquez, K. M. Kaye, The internal Kaposi's sarcoma-associated herpesvirus
472 LANA regions exert a critical role on episome persistence. *J Virol* **85**, 7622-7633 (2011).
473 10. A. J. Barbera *et al.*, The Nucleosomal Surface as a Docking Station for Kaposi's Sarcoma
474 Herpesvirus LANA. *Science (New York, N.Y* **311**, 856-861 (2006).
475 11. S. Matsumura, L. M. Persson, L. Wong, A. C. Wilson, The latency-associated nuclear
476 antigen interacts with MeCP2 and nucleosomes through separate domains. *J Virol* **84**,
477 2318-2330 (2010).
478 12. A. Krithivas, M. Fujimuro, M. Weidner, D. B. Young, S. D. Hayward, Protein interactions
479 targeting the latency-associated nuclear antigen of Kaposi's sarcoma-associated
480 herpesvirus to cell chromosomes. *J Virol* **76**, 11596-11604 (2002).
481 13. A. Viejo-Borbolla *et al.*, Brd2/RING3 interacts with a chromatin-binding domain in the
482 Kaposi's Sarcoma-associated herpesvirus latency-associated nuclear antigen 1 (LANA-1)
483 that is required for multiple functions of LANA-1. *J Virol* **79**, 13618-13629 (2005).
484 14. J. Hellert *et al.*, The 3D structure of Kaposi sarcoma herpesvirus LANA C-terminal domain
485 bound to DNA. *Proceedings of the National Academy of Sciences of the United States of*
486 *America* **112**, 6694-6699 (2015).
487 15. A. C. Garber, J. Hu, R. Renne, Latency-associated nuclear antigen (LANA) cooperatively
488 binds to two sites within the terminal repeat, and both sites contribute to the ability of
489 LANA to suppress transcription and to facilitate DNA replication. *J Biol Chem* **277**, 27401-
490 27411 (2002).
491 16. J. F. Domsic, H. S. Chen, F. Lu, R. Marmorstein, P. M. Lieberman, Molecular basis for
492 oligomeric-DNA binding and episome maintenance by KSHV LANA. *PLoS Pathog* **9**,
493 e1003672 (2013).
494 17. A. De Leo *et al.*, LANA oligomeric architecture is essential for KSHV nuclear body
495 formation and viral genome maintenance during latency. *PLoS Pathog* **15**, e1007489
496 (2019).
497 18. J. M. Hall, D. P. McDonnell, K. S. Korach, Allosteric regulation of estrogen receptor
498 structure, function, and coactivator recruitment by different estrogen response elements.
499 *Molecular endocrinology (Baltimore, Md* **16**, 469-486 (2002).
500 19. X. Nan, F. J. Campoy, A. Bird, MeCP2 is a transcriptional repressor with abundant binding
501 sites in genomic chromatin. *Cell* **88**, 471-481 (1997).
502 20. P. L. Jones *et al.*, Methylated DNA and MeCP2 recruit histone deacetylase to repress
503 transcription. *Nature genetics* **19**, 187-191 (1998).
504 21. X. Nan *et al.*, Transcriptional repression by the methyl-CpG-binding protein MeCP2
505 involves a histone deacetylase complex. *Nature* **393**, 386-389 (1998).
506 22. A. J. Bannister *et al.*, Selective recognition of methylated lysine 9 on histone H3 by the
507 HP1 chromo domain. *Nature* **410**, 120-124 (2001).
508 23. M. Lachner, D. O'Carroll, S. Rea, K. Mechtler, T. Jenuwein, Methylation of histone H3
509 lysine 9 creates a binding site for HP1 proteins. *Nature* **410**, 116-120 (2001).

510 24. N. Agarwal *et al.*, MeCP2 interacts with HP1 and modulates its heterochromatin
511 association during myogenic differentiation. *Nucleic acids research* **35**, 5402-5408 (2007).
512 25. M. L. Gonzales, S. Adams, K. W. Dunaway, J. M. LaSalle, Phosphorylation of distinct
513 sites in MeCP2 modifies cofactor associations and the dynamics of transcriptional
514 regulation. *Molecular and cellular biology* **32**, 2894-2903 (2012).
515 26. M. Jinek *et al.*, A programmable dual-RNA-guided DNA endonuclease in adaptive
516 bacterial immunity. *Science (New York, N.Y* **337**, 816-821 (2012).
517 27. L. S. Qi *et al.*, Repurposing CRISPR as an RNA-guided platform for sequence-specific
518 control of gene expression. *Cell* **152**, 1173-1183 (2013).
519 28. L. A. Gilbert *et al.*, CRISPR-mediated modular RNA-guided regulation of transcription in
520 eukaryotes. *Cell* **154**, 442-451 (2013).
521 29. W. Deng, X. Shi, R. Tjian, T. Lionnet, R. H. Singer, CASFISH: CRISPR/Cas9-mediated
522 in situ labeling of genomic loci in fixed cells. *Proceedings of the National Academy of*
523 *Sciences of the United States of America* **112**, 11870-11875 (2015).
524 30. B. Chen *et al.*, Dynamic imaging of genomic loci in living human cells by an optimized
525 CRISPR/Cas system. *Cell* **155**, 1479-1491 (2013).
526 31. T. Anton, S. Bultmann, H. Leonhardt, Y. Markaki, Visualization of specific DNA
527 sequences in living mouse embryonic stem cells with a programmable fluorescent
528 CRISPR/Cas system. *Nucleus* **5**, 163-172 (2014).
529 32. J. Duan *et al.*, Live imaging and tracking of genome regions in CRISPR/dCas9 knock-in
530 mice. *Genome Biol* **19**, 192 (2018).
531 33. M. E. Tanenbaum, L. A. Gilbert, L. S. Qi, J. S. Weissman, R. D. Vale, A protein-tagging
532 system for signal amplification in gene expression and fluorescence imaging. *Cell* **159**,
533 635-646 (2014).
534 34. M. E. Ballestas, P. A. Chatis, K. M. Kaye, Efficient persistence of extrachromosomal
535 KSHV DNA mediated by latency-associated nuclear antigen. *Science (New York, N.Y* **284**,
536 641-644 (1999).
537 35. B. Kelley-Clarke *et al.*, Determination of Kaposi's sarcoma-associated herpesvirus C-
538 terminal latency-associated nuclear antigen residues mediating chromosome association
539 and DNA binding. *J Virol* **81**, 4348-4356 (2007).
540 36. J. Hellert *et al.*, A structural basis for BRD2/4-mediated host chromatin interaction and
541 oligomer assembly of Kaposi sarcoma-associated herpesvirus and murine
542 gammaherpesvirus LANA proteins. *PLoS Pathog* **9**, e1003640 (2013).
543 37. W. Stedman, Z. Deng, F. Lu, P. M. Lieberman, ORC, MCM, and Histone Hyperacetylation
544 at the Kaposi's Sarcoma-Associated Herpesvirus Latent Replication Origin. *J. Virol.* **78**,
545 12566-12575 (2004).
546 38. S. C. Verma, K. Lan, T. Choudhuri, M. A. Cotter, E. S. Robertson, An autonomous
547 replicating element within the KSHV genome. *Cell host & microbe* **2**, 106-118 (2007).
548 39. A. Krithivas, D. B. Young, G. Liao, D. Greene, S. D. Hayward, Human herpesvirus 8
549 LANA interacts with proteins of the mSin3 corepressor complex and negatively regulates
550 Epstein-Barr virus gene expression in dually infected PEL cells. *J Virol* **74**, 9637-9645
551 (2000).
552 40. Q. Cai *et al.*, A unique SUMO-2-interacting motif within LANA is essential for KSHV
553 latency. *PLoS Pathog* **9**, e1003750 (2013).

554 41. S. C. Verma, Q. Cai, E. Kreider, J. Lu, E. S. Robertson, Comprehensive analysis of LANA
555 interacting proteins essential for viral genome tethering and persistence. *PloS one* **8**,
556 e74662 (2013).
557 42. G. Stuber *et al.*, HHV-8 encoded LANA-1 alters the higher organization of the cell nucleus.
558 *Molecular cancer* **6**, 28 (2007).
559 43. I. Rhee *et al.*, DNMT1 and DNMT3b cooperate to silence genes in human cancer cells.
560 *Nature* **416**, 552-556 (2002).
561 44. R. P. Ghosh, R. A. Horowitz-Scherer, T. Nikitina, L. M. Gierasch, C. L. Woodcock, Rett
562 syndrome-causing mutations in human MeCP2 result in diverse structural changes that
563 impact folding and DNA interactions. *J Biol Chem* **283**, 20523-20534 (2008).
564 45. J. Traynor, P. Agarwal, L. Lazzeroni, U. Francke, Gene expression patterns vary in clonal
565 cell cultures from Rett syndrome females with eight different MECP2 mutations. *BMC*
566 *Med Genet* **3**, 12 (2002).
567 46. R. Griffiths, A. Whitehouse, Herpesvirus saimiri episomal persistence is maintained via
568 interaction between open reading frame 73 and the cellular chromosome-associated protein
569 MeCP2. *J Virol* **81**, 4021-4032 (2007).
570 47. P. C. Dedon, J. A. Soults, C. D. Allis, M. A. Gorovsky, A simplified formaldehyde fixation
571 and immunoprecipitation technique for studying protein-DNA interactions. *Anal Biochem*
572 **197**, 83-90 (1991).
573 48. V. Orlando, R. Paro, Mapping Polycomb-repressed domains in the bithorax complex using
574 in vivo formaldehyde cross-linked chromatin. *Cell* **75**, 1187-1198 (1993).
575 49. A. S. Gonzalez-Serricchio, P. W. Sternberg, Visualization of C. elegans transgenic arrays
576 by GFP. *BMC Genet* **7**, 36 (2006).
577 50. M. Higa *et al.*, TRF2 recruits ORC through TRFH domain dimerization. *Biochim Biophys*
578 *Acta Mol Cell Res* **1864**, 191-201 (2017).
579 51. Y. Gao, M. Han, S. Shang, H. Wang, L. S. Qi, Interrogation of the dynamic properties of
580 higher-order heterochromatin using CRISPR-dCas9. *Molecular cell*
581 10.1016/j.molcel.2021.07.034 (2021).
582 52. Y. Shin *et al.*, Liquid Nuclear Condensates Mechanically Sense and Restructure the
583 Genome. *Cell* **175**, 1481-1491 e1413 (2018).
584 53. O. Vladimirova *et al.*, Phase separation and DAXX redistribution contribute to LANA
585 nuclear body and KSHV genome dynamics during latency and reactivation. *PLoS Pathog*
586 **17**, e1009231 (2021).
587 54. L. Wang *et al.*, Rett syndrome-causing mutations compromise MeCP2-mediated liquid-
588 liquid phase separation of chromatin. *Cell Res* **30**, 393-407 (2020).
589 55. M. Calderwood, R. E. White, R. A. Griffiths, A. Whitehouse, Open reading frame 73 is
590 required for herpesvirus saimiri A11-S4 episomal persistence. *J Gen Virol* **86**, 2703-2708
591 (2005).
592 56. M. Girard *et al.*, Parental origin of de novo MECP2 mutations in Rett syndrome. *Eur J*
593 *Hum Genet* **9**, 231-236 (2001).
594 57. R. Trappe *et al.*, MECP2 mutations in sporadic cases of Rett syndrome are almost
595 exclusively of paternal origin. *Am J Hum Genet* **68**, 1093-1101 (2001).
596 58. V. H. Adams, S. J. McBryant, P. A. Wade, C. L. Woodcock, J. C. Hansen, Intrinsic disorder
597 and autonomous domain function in the multifunctional nuclear protein, MeCP2. *J Biol*
598 *Chem* **282**, 15057-15064 (2007).

59. R. P. Ghosh, R. A. Horowitz-Scherer, T. Nikitina, L. S. Shlyakhtenko, C. L. Woodcock, MeCP2 binds cooperatively to its substrate and competes with histone H1 for chromatin binding sites. *Molecular and cellular biology* **30**, 4656-4670 (2010).
60. M. Fujimuro, S. D. Hayward, The latency-associated nuclear antigen of Kaposi's sarcoma-associated herpesvirus manipulates the activity of glycogen synthase kinase-3beta. *J Virol* **77**, 8019-8030 (2003).
61. S. Morita *et al.*, Targeted DNA demethylation in vivo using dCas9-peptide repeat and scFv-TET1 catalytic domain fusions. *Nature biotechnology* **34**, 1060-1065 (2016).
62. B. W. Stringer *et al.*, A reference collection of patient-derived cell line and xenograft models of proneural, classical and mesenchymal glioblastoma. *Sci Rep* **9**, 4902 (2019).
63. M. Shamay, M. Greenway, G. Liao, R. F. Ambinder, S. D. Hayward, De novo DNA methyltransferase DNMT3b interacts with NEDD8-modified proteins. *J Biol Chem* **285**, 36377-36386 (2010).
64. J. Myoung, D. Ganem, Infection of lymphoblastoid cell lines by Kaposi's sarcoma-associated herpesvirus: critical role of cell-associated virus. *J Virol* **85**, 9767-9777 (2011).
65. C. A. Schneider, W. S. Rasband, K. W. Eliceiri, NIH Image to ImageJ: 25 years of image analysis. *Nat Methods* **9**, 671-675 (2012).
66. A. Free *et al.*, DNA recognition by the methyl-CpG binding domain of MeCP2. *J Biol Chem* **276**, 3353-3360 (2001).

634 **Figure legends**

635 **Figure 1. Schematic illustration of CRISPR-PITA. (A)** Schematic illustration of dCas9-SunTag, sgRNA
636 and scFv-LANA or other protein of interest (scFv-pY), and their binding to repetitive elements. **(B)** SLK
637 cells were transfected with dCas9-SunTag, scFv-LANA, and sgTelomere as illustrated on the left of the
638 images. Immunofluorescence assay was performed to detect LANA (red), and the nucleus was stained with
639 DAPI (blue). Scale bar = 5 μm. **(C)** Schematic illustration of the CRISPR-PITA, targeting of scFv-LANA
640 or any other protein of interest to the telomeres via dCas9. Then the recruitment of other nuclear proteins
641 to these dots is evaluated via immunostaining.

642 **Figure 2. LANA recruits ORC2 and SIN3A but not MeCP2.** SLK cells were transfected with dCas9-
643 SunTag, scFv-LANA, and sgTelomere expression plasmids as can be seen in the illustrations on the left.
644 Immunofluorescence assays were performed to detect LANA (red) and ORC2 **(A)** mSin3a **(B)** or MeCP2
645 **(C)** (in green) cellular localization. The nucleus was stained with DAPI. Scale bar = 5 μm. The plots of the
646 red, green and blue pixel intensities along the white arrow (in the left panels) are presented. (**D**) Pearson's
647 correlation coefficient was determined by ImageJ (JACoP Pluing) (65) for 15 different cells in each
648 treatment, and presented as box and whiskers (min to max). One-tailed *t* tests were performed (*, $P \leq 0.05$;
649 **, $P \leq 0.01$; ***; $P \leq 0.001$).

650 **Figure 3. MeCP2 recruits LANA.** SLK cells were transfected with dCas9-SunTag, scFv-MeCP2, and
651 sgTelomere in combination with GFP-LANA **(A)** or GFP **(B)** as illustrated on the left. Immunofluorescence
652 assay was performed to detect scFv-MeCP2, or fluorescently labelled GFP-LANA and GFP. The nucleus
653 was stained with DAPI. Scale bar = 5 μm. The plots of the red, green and blue pixel intensities along the
654 white arrow (in the left panels) are presented. (**C**) SLK cells were transfected with FLAG-LANA N+C,
655 FLAG-LANA C, or FLAG-LANA N, same as in A. Immunofluorescence assay was performed to detect
656 both scFv-MeCP2 and LANA. (**D**) ChIP assay to detect LANA (left panel) and MeCP2 (right panel)
657 association with the ERBB2 promoter following recruitment with sgRNA to this locus.

658 **Figure 4. MeCP2 recruits HDAC1, while HDAC1 cannot recruit MeCP2. (A)** HCT cells were
659 transfected with dCas9-SunTag, scFv-MeCP2 and sgTelomere as illustrated on the left.
660 Immunofluorescence assay was performed to detect HDAC1 (green) and scFv-MeCP2 (red). **(B-C)** HCT
661 **(B)** and HCT DKO **(C)** cells were transfected same as in A but with scFv-HDAC1. Immunofluorescence
662 assay was performed to detect MeCP2 (green) and scFv-HDAC1 (red). The nucleus was stained with DAPI.
663 Scale bar = 5 μm. The plots of the red, green and blue pixel intensities along the white arrow (in the left
664 panels) are presented.

665 **Figure 5. Availability of interacting domains determines recruitment directionality.** (**A**) schematic
666 presentation of MeCP2 and the interaction domains with LANA, HDAC1, and HP1α. Two Rett syndrome
667 mutants are indicated above. (**B**) SLK cells were transfected with dCas9-SunTag, scFv-HP1α, and
668 sgTelomere as illustrated on the left. Immunofluorescence assay was performed to detect MeCP2 (green)
669 and scFv-HP1α (red). The nucleus was stained with DAPI. Scale bar = 5 μm. Schematic illustrations of the
670 model for free (**C**) and DNA bound (**D**) MeCP2 are presented. (**E**) Schematic presentation of the experiment
671 in (**F**). (**F**) SLK cells were transfected with dCas9-SunTag, scFv-LANA, and sgTelomere. The next day
672 they were kept un-transfected or transfected with MeCP2 site binding oligo (66), or control Oligo.
673 Immunofluorescence assay was performed to detect MeCP2 (green) and scFv-LANA (red). The plots of
674 the red, green and blue pixel intensities along the white arrow (in the left panels) are presented.

675 **Figure 6. Rett syndrome mutant MeCP2 T158M cannot support KSHV latency. (A-B)** LCLs were
676 infected with rKSHV.219 and GFP-positive cells by FACS analysis (**A**) or amount of KSHV DNA by
677 qPCR (**B**) were evaluated at the indicated time points. Experiments were performed with biological
678 triplicates. (**C**) Immunofluorescence assay was performed to detect GFP-LANA (green) and scFv- MeCP2
679 (red). The nucleus was stained with DAPI. Scale bar = 5 μm. (**D**) NIH 3T3 cells were transfected with
680 GFP-LANA and wt MeCP2, T158M mutant, or del-MBD. Immunofluorescence assay was performed same
681 as in C. The plots of the red, green and blue pixel intensities along the white arrow (in the left panels) are
682 presented.

683

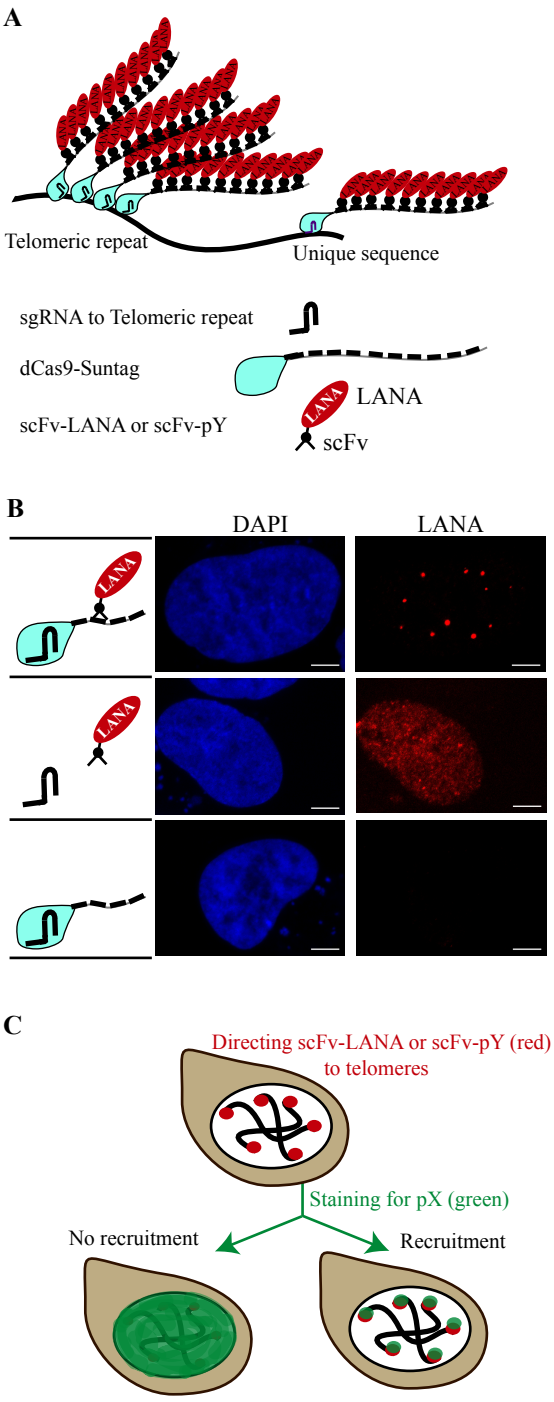
A
Telomeric repeat
Unique sequence
sgRNA to Telomeric repeat
dCas9-Suntag
scFv-LANA or scFv-pY
LANA
scFv
B
DAPI
LANA
C
Directing scFv-LANA or scFv-pY (red)
to telomeres
Staining for pX (green)
No recruitment
Recruitment

Fig.1

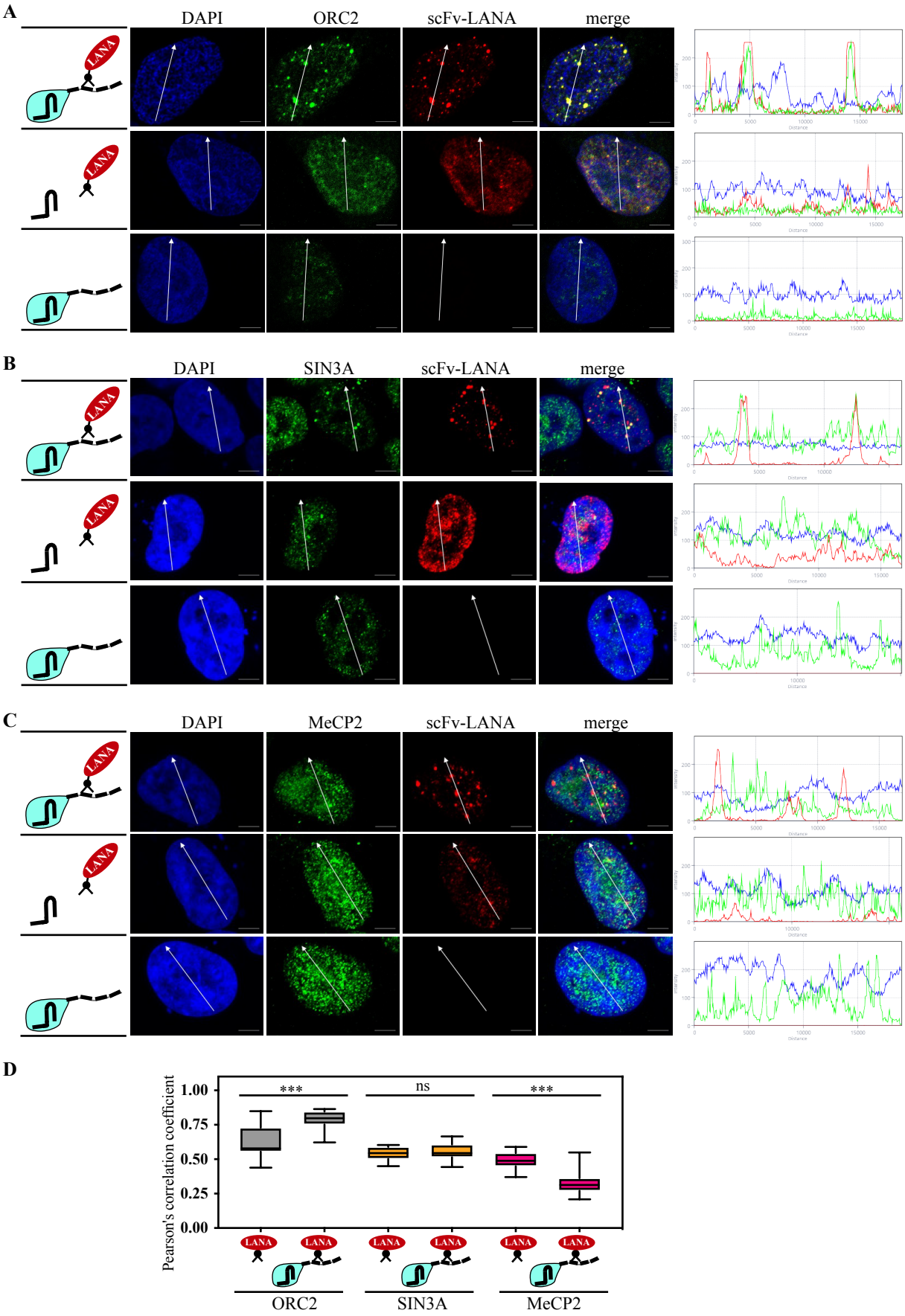
A
DAPI
ORC2
scFv-LANA
merge
LANA
B
DAPI
SIN3A
scFv-LANA
merge
LANA
C
DAPI
MeCP2
scFv-LANA
merge
LANA
D
Pearson's correlation coefficient
1.00
0.75
0.50
0.25
0.00
***
ns
***
LANA
ORC2
SIN3A
MeCP2

Fig.2

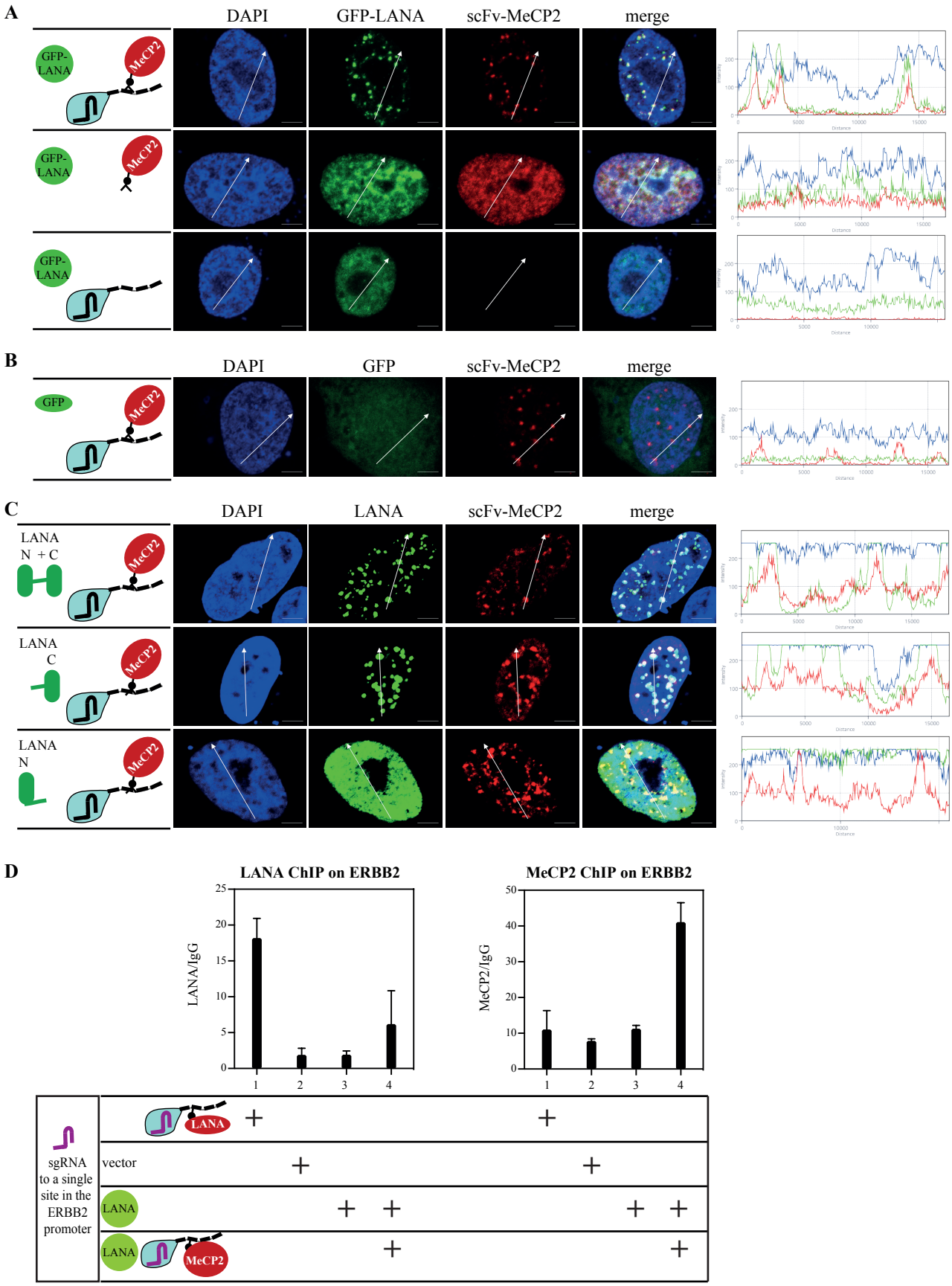
A
DAPI
GFP-LANA
scFv-MeCP2
merge
GFP-LANA
MeCP2
B
DAPI
GFP
scFv-MeCP2
merge
GFP
MeCP2
C
DAPI
LANA
scFv-MeCP2
merge
LANA N + C
LANA C
LANA N
MeCP2
D
LANA ChIP on ERBB2
LANA/IgG
MeCP2 ChIP on ERBB2
MeCP2/IgG
sgRNA to a single site in the ERBB2 promoter
LANA
vector
MeCP2

Fig.3

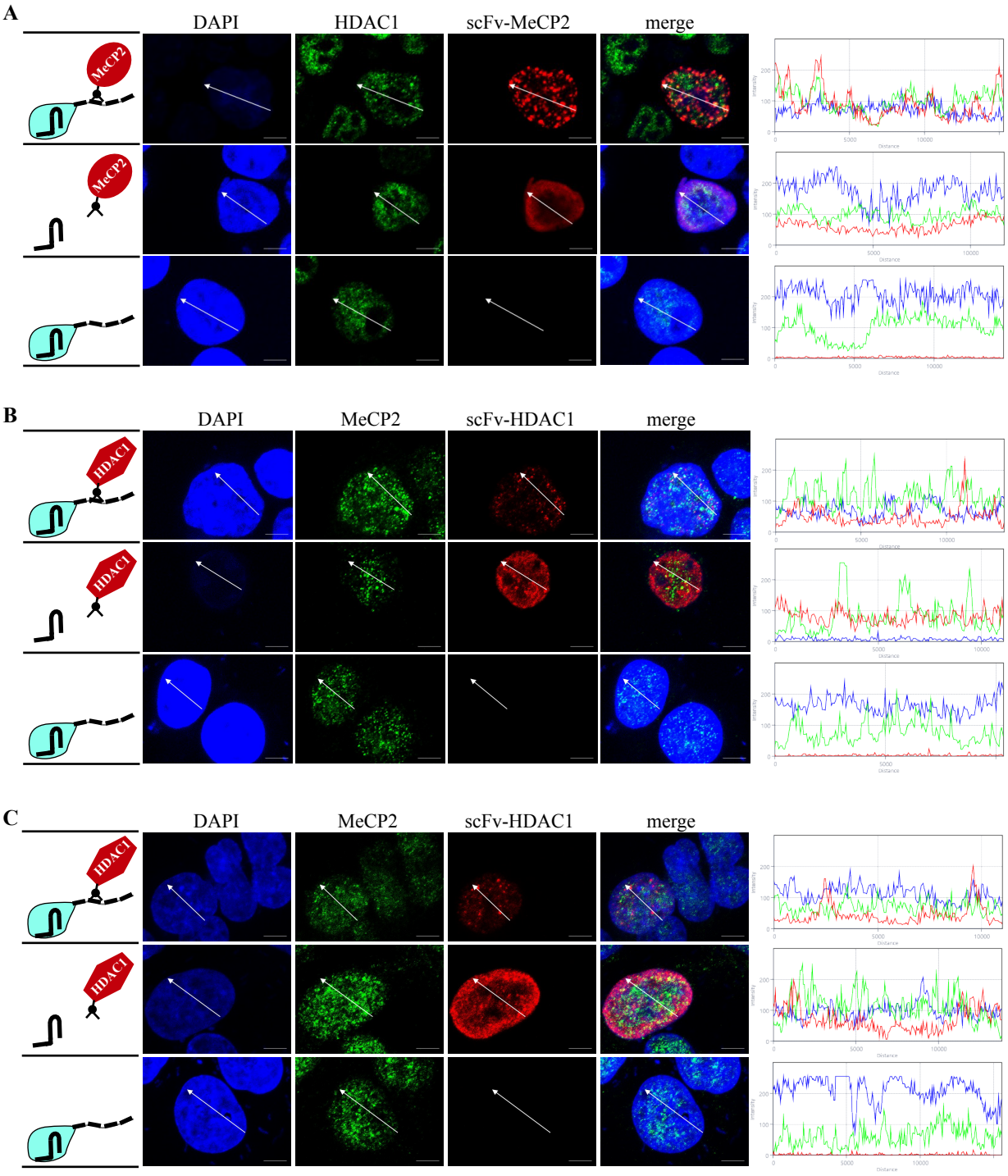
A
DAPI
HDAC1
scFv-MeCP2
merge
MeCP2
MeCP2
B
DAPI
MeCP2
scFv-HDAC1
merge
HDAC1
HDAC1
C
DAPI
MeCP2
scFv-HDAC1
merge
HDAC1
HDAC1

Fig.4

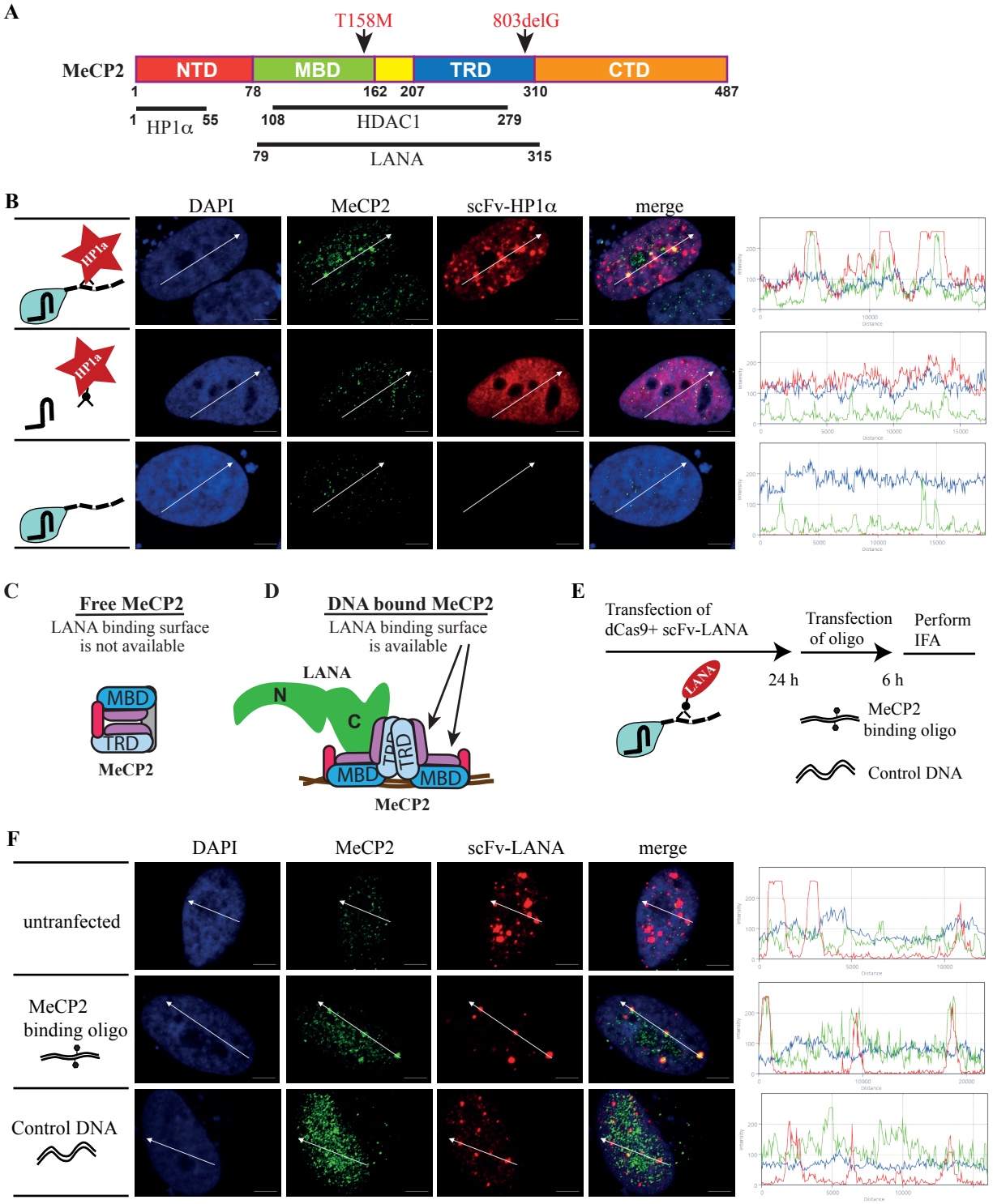
A
T158M
803delG
MeCP2
NTD
MBD
TRD
CTD
1
78
162
207
310
487
1
HP1α
55
108
HDAC1
279
79
LANA
315
B
DAPI
MeCP2
scFv-HP1α
merge
HP1a
C
Free MeCP2
LANA binding surface
is not available
MBD
TRD
MeCP2
D
DNA bound MeCP2
LANA binding surface
is available
LANA
N
C
TRD
MBD
MBD
MeCP2
E
Transfection of
dCas9+ scFv-LANA
Transfection
of oligo
Perform
IFA
24 h
6 h
LANA
MeCP2
binding oligo
Control DNA
F
DAPI
MeCP2
scFv-LANA
merge
untranfected
MeCP2
binding oligo
Control DNA

Fig.5

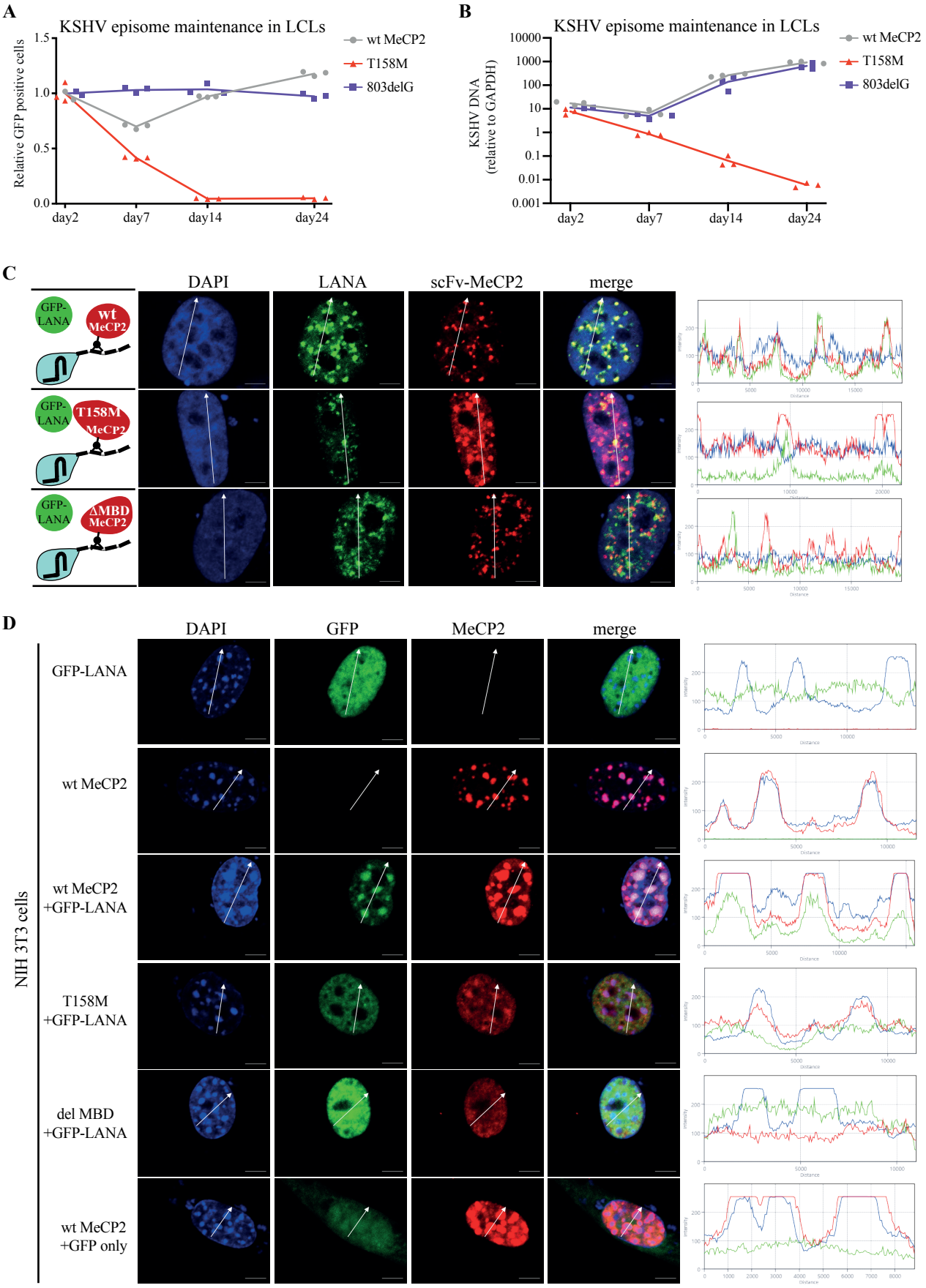
A
KSHV episome maintenance in LCLs
Relative GFP positive cells
1.5
1.0
0.5
0.0
day2
day7
day14
day24
wt MeCP2
T158M
803delG
B
KSHV episome maintenance in LCLs
KSHV DNA
(relative to GAPDH)
10000
1000
100
10
1
0.1
0.01
0.001
day2
day7
day14
day24
wt MeCP2
T158M
803delG
C
DAPI
LANA
scFv-MeCP2
merge
GFP-LANA
wt MeCP2
GFP-LANA
T158M MeCP2
GFP-LANA
ΔMBD MeCP2
D
DAPI
GFP
MeCP2
merge
NIH 3T3 cells
GFP-LANA
wt MeCP2
wt MeCP2
+GFP-LANA
T158M
+GFP-LANA
del MBD
+GFP-LANA
wt MeCP2
+GFP only

Fig.6